Differential settlements due to cyclic loading and their effect on the lifetime of structures

T. Wichtmann, A. Niemunis & Th. Triantafyllidis
Institute for Soil Mechanics and Rock Mechanics, University of Karlsruhe, Germany

Keywords: sand, cyclic loading, accumulation, differential settlement, high-cycle model

ABSTRACT: The paper briefly summarizes a study on the accumulation phenomenon in sand due to cyclic loading. Most of the experimental findings have been implemented into a high-cycle accumulation (HCA) model for sand. The model predicts permanent deformations in non-cohesive soils due to many cycles ($N > 10^3$) with relatively small amplitudes ($\varepsilon^{\text{ampl}} < 10^{-3}$). The paper discusses the most recent experimental results and developments of the HCA model. It is demonstrated that Miner's rule is applicable to granular soils as a first approximation. In order to develop a simplified procedure for the determination of the material constants of the HCA model an extensive testing program was carried out to correlate the constants with index properties. In another test series the behaviour of sand under drained and undrained cyclic loading were compared in order to develop a suitable "elastic" stiffness E in the basic HCA equation $\dot{\boldsymbol{\sigma}} = \mathsf{E} : (\dot{\boldsymbol{\varepsilon}} - \dot{\boldsymbol{\varepsilon}}^{\text{acc}})$. The paper also summarizes new ideas for an amplitude definition for complex 6-dimensional strain loops. A FE study of a statically indeterminate structure on an inhomogeneous subsoil is presented. A positive feedback between the settlement and the settlement rate is demonstrated.

1 INTRODUCTION

The high-cycle accumulation (HCA) model recently proposed by the authors (Niemunis et al., 2005b) predicts permanent deformations (pseudo-creep) or changes of stress (pseudo-relaxation) in non-cohesive soils due to many cycles ($N > 10^3$) with relatively small amplitudes ($\varepsilon^{\text{ampl}} < 10^{-3}$), so-called high- or polycyclic loading. The model is based on an extensive laboratory testing program (Wichtmann, 2005; Wichtmann et al., 2005a, 2006a, 2007a,b). An outline of the HCA model is given in Section 2. Typically, the model can be applied to foundations subjected to traffic loading, to wind power plants, to machine foundations and to problems related to mechanical compaction of granular soils.

In many practical problems the amplitude of the cycles is not constant but varies with each cycle. Such random cyclic loadings could be replaced by packages of cycles each with a constant amplitude, if the sequence of application of the packages would not affect the final residual strain, that means if Miner's rule (Miner, 1945) were applicable to soil. An experimental study of Miner's rule for sand is presented in Section 3.

Up to the present, the determination of the material constants of the high-cycle model is laborious. Nine cyclic triaxial tests each with a duration of at least half a week (10^5 cycles at a frequency of 1 Hz) are necessary and sophisticated test devices are indispensable. In order to develop a simplified procedure, the material constants of eight different grain size distribution curves of a quartz sand have been determined in approx. 200 cyclic triaxial tests. Correlations between the material constants and index properties have been proposed and verified. The test results, possible correlation formulas and an approach for a simplified calibration procedure are presented in Section 4.

A major novel finding wrt (Niemunis et al., 2005b) is a peculiar variability of the "elastic" stiffness

E in the basic equation $\dot{\boldsymbol{\sigma}} = \mathsf{E} : (\dot{\boldsymbol{\varepsilon}} - \dot{\boldsymbol{\varepsilon}}^{\text{acc}})$ of the model with the number of cycles N. E interrelates the pseudo-creep $\dot{\boldsymbol{\varepsilon}} = \dot{\boldsymbol{\varepsilon}}^{\text{acc}}$ and the pseudo-relaxation $\dot{\boldsymbol{\sigma}} = -\mathsf{E} : \dot{\boldsymbol{\varepsilon}}^{\text{acc}}$. While the rate of strain accumulation $\dot{\boldsymbol{\varepsilon}}^{\text{acc}}$ was extensively studied in drained cyclic triaxial tests, relatively sparse information is available on E. For some BVPs in which considerable changes of the average stress are expected, a closer inspection of E becomes necessary. An experimental study of E is described in Section 5.

If several sources of cyclic loading are acting simultaneously, complex strain loops may result from different polarizations and frequencies of the cycles. A procedure for the determination of the strain amplitude and the number of cycles as input variables for the HCA model is discussed in Section 6.

A FE study showing a positive feedback effect for a statically indeterminate structure on an inhomogeneous soil (stochastically distributed void ratio) is documented in Section 7.

2 HIGH-CYCLE MODEL

The basic assumption of the high-cycle model recently proposed by the authors (Niemunis et al., 2005b) is that the strain path and the stress path resulting from a cyclic loading can be decomposed into an oscillating part and a trend and that both can be treated separately. The oscillating part is described by the strain amplitude. The model predicts the trend (accumulation) of strain $\dot{\boldsymbol{\varepsilon}}^{\text{acc}}$ only. Depending on the boundary conditions, the trend of stress or of strain can be observed. They are interrelated by

$$\dot{\boldsymbol{\sigma}} = \mathsf{E} : (\dot{\boldsymbol{\varepsilon}} - \dot{\boldsymbol{\varepsilon}}^{\text{acc}} - \dot{\boldsymbol{\varepsilon}}^{\text{pl}}) \tag{1}$$

with the objective Jaumann stress rate $\dot{\boldsymbol{\sigma}}$ of the effective stress $\boldsymbol{\sigma}$ (compression positive), the strain rate $\dot{\boldsymbol{\varepsilon}}$ (compression positive), the given accumulation rate $\dot{\boldsymbol{\varepsilon}}^{\text{acc}}$, a plastic strain rate $\dot{\boldsymbol{\varepsilon}}^{\text{pl}}$ (for stress paths touching the yield surface due to an accompanying monotonous loading) and a barotropic elastic stiffness E. In the context of high-cycle models "rate" means a derivative with respect to the number of cycles N (instead of time t), i.e. $\dot{\sqcup} = \partial \sqcup / \partial N$. For $\dot{\boldsymbol{\varepsilon}}^{\text{acc}}$ in Eq. (1)

$$\dot{\boldsymbol{\varepsilon}}^{\text{acc}} \;=\; \dot{\varepsilon}^{\text{acc}}\, \mathbf{m} \tag{2}$$

is used with the flow rule $\mathbf{m} = \dot{\boldsymbol{\varepsilon}}^{\text{acc}} / \|\dot{\boldsymbol{\varepsilon}}^{\text{acc}}\|$ (unit tensor) and the flow intensity $\dot{\varepsilon}^{\text{acc}} = \|\dot{\boldsymbol{\varepsilon}}^{\text{acc}}\|$. The flow rule of the modified Cam clay (MCC) model

$$\mathbf{m} \;=\; \left[\frac{1}{3}\left(p - \frac{q^2}{M^2 p}\right)\mathbf{1} + \frac{3}{M^2}\boldsymbol{\sigma}^*\right]^{\rightarrow} \tag{3}$$

approximates well the ratios $\dot{\varepsilon}_v^{\text{acc}} / \dot{\varepsilon}_q^{\text{acc}}$ measured in drained cyclic triaxial tests ($\dot{\varepsilon}_v$, $\dot{\varepsilon}_q$ = rates of volumetric or deviatoric strain, respectively). The superposed arrow denotes Euclidean normalization, $\sqcup^*$ means the deviatoric part of $\sqcup$ and p,q are Roscoe's invariants. For the triaxial case $p = (\sigma_1 + 2\sigma_3)/3$ and $q = \sigma_1 - \sigma_3$ holds. For triaxial extension ($\eta = q/p < 0$) a small modification $M = F\, M_c$ is used with $F = 1 + M_e/3$ for $\eta \le M_e$, $F = 1 + \eta/3$ for $M_e < \eta < 0$ and $F = 1$ for $\eta \ge 0$ wherein $M_c = 6\sin\varphi_c/(3 - \sin\varphi_c)$ and $M_e = -6\sin\varphi_c/(3 + \sin\varphi_c)$. The intensity of strain accumulation $\dot{\varepsilon}^{\text{acc}}$ in Eq. (2) is calculated as a product of six functions:

$$\dot{\varepsilon}^{\text{acc}} \;=\; f_{\text{ampl}}\, \dot{f}_N\, f_e\, f_p\, f_Y\, f_\pi \tag{4}$$

Each function considers the influence of a different parameter (see Table 1). For a detailed description of f_π it is referred to Niemunis et al. (2005b). The model incorporates a tensorial definition of the amplitude for multidimensional strain loops (Niemunis et al., 2005b) (a procedure for more complex

Table 1: Summary of the functions, material constants and reference quantities of the high-cycle model

Influencing parameter	Function	Material constants	Reference quantities
Strain amplitude	$f_{\text{ampl}} = \min\left[\left(\frac{\varepsilon^{\text{ampl}}}{\varepsilon^{\text{ampl}}_{\text{ref}}}\right)^2; 100\right]$		$\varepsilon^{\text{ampl}}_{\text{ref}} = 10^{-4}$
Cyclic preloading	$\dot{f}_N = \dot{f}_N^A + \dot{f}_N^B$ $\dot{f}_N^A = C_{N1}C_{N2}\exp\left[-\frac{g^A}{C_{N1}\, f_{\text{ampl}}}\right]$ $\dot{f}_N^B = C_{N1}C_{N3}$	C_{N1} C_{N2} C_{N3}	
Average mean pressure	$f_p = \exp\left[-C_p\left(\frac{p^{\text{av}}}{p_{\text{ref}}} - 1\right)\right]$	C_p	p_{ref} = 100 kPa
Average stress ratio	$f_Y = \exp\left(C_Y\, \bar{Y}^{\text{av}}\right)$	C_Y	
Void ratio	$f_e = \frac{(C_e-e)^2}{1+e}\,\frac{1+e_{\text{ref}}}{(C_e-e_{\text{ref}})^2}$	C_e	$e_{\text{ref}} = e_{\max}$

strain loops is proposed in Section 6). The number of cycles is weighted with their amplitude, i.e. the "cyclic preloading" can be quantified with the historiotropic variable g^A defined via the following evolution equation:

$$\dot{g}^A = f_{\text{ampl}} C_{N1} C_{N2} \exp[-g^A/(C_{N1} f_{\text{ampl}})] \tag{5}$$

3 IS MINER'S RULE APPLICABLE TO SOIL?

In order to study the applicability of Miner's rule to sand cyclic triaxial tests have been performed (Wichtmann, 2005; Wichtmann et al., 2006b). In each test four packages each with 25,000 cycles were applied. The amplitudes q^{ampl} = 20, 40, 60 and 80 kPa were arranged in six different sequences (Figure 1a). Figure 1b presents the accumulation curves $\varepsilon^{\text{acc}}(N)$. The residual strains at the end of the tests (i.e. at $N = 10^5$) are quite similar. The differences result mainly from the fact that the cycles affect the stiffness during a subsequent monotonic loading (Wichtmann, 2005; Wichtmann et al., 2006b). Thus, the residual strain accumulated in the first cycle of each package depends on the previous amplitudes, i.e. on the sequence of application of the packages. For a constant polarization of the cycles and as a first approximation, Miner's rule can be assumed valid for sand and the influence of the sequence of application can be neglected. In the HCA model, Miner's rule is obeyed by the usage of the historiotropic variable g^A. As demonstrated in (Wichtmann, 2005; Wichtmann et al., 2006b) the curves $\varepsilon^{\text{acc}}(N)$ shown in Figure 1b are well approximated by the HCA model.

4 CORRELATION OF MATERIAL CONSTANTS WITH GRANULOMETRIC PROPERTIES

In order to develop a simplified procedure for the determination of the material constants of the HCA model eight grain size distribution curves (Fig. 2) of a quartz sand with sub-angular grain shape have been tested. They differed in the mean grain size d_{50} and in the uniformity coefficient $C_u = d_{60}/d_{10}$. The high-cycle model was first developed using test results for the medium coarse to coarse sand No. 3. Approximately 200 cyclic triaxial tests were performed in the present study. For each sand the stress amplitude q^{ampl}, the average mean pressure p^{av}, the average stress ratio η^{av} and the initial void ratio e_0 were varied.

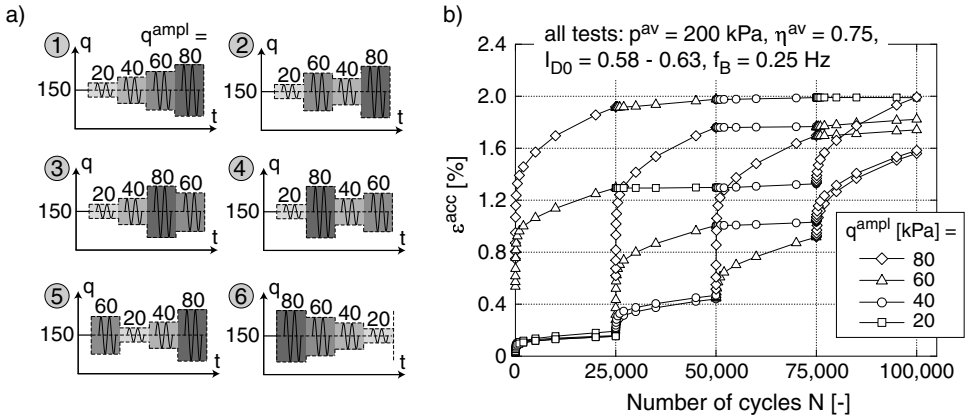

Fig. 1: *Tests with packages of cycles with different amplitudes arranged in different sequences ($I_D = (e_{\max} - e)/(e_{\max} - e_{\min})$; I_{D0} = initial value prior to cyclic loading)*

The test results (documented in more detail by Wichtmann et al. (2007c)) on the seven additionally tested grain size distribution curves (Nos. 1,2,4-8) confirm the main conclusions from the tests on sand No. 3 (Wichtmann, 2005), i.e. the "cyclic flow rule" $\dot{\varepsilon}_v^{\text{acc}}/\dot{\varepsilon}_q^{\text{acc}}$, the proportionality between the accumulation rate $\dot{\varepsilon}^{\text{acc}}$ and the square of the strain amplitude $(\bar{\varepsilon}^{\text{ampl}})^2$ and the increase of $\dot{\varepsilon}^{\text{acc}}$ with increasing void ratio, with decreasing average mean pressure p^{av} and with increasing average stress ratio $\eta^{\text{av}} = q^{\text{av}}/p^{\text{av}}$. However, the intensity of accumulation depends strongly on d_{50} and C_u (Figure 2). Furthermore, a change of the shape of the curves $\varepsilon^{\text{acc}}(N)$, i.e. an increase of the linear portion of the function f_N of the HCA model, with C_u was observed.

The constants C_e, C_p, C_Y, C_{N1}, C_{N2} and C_{N3} of the HCA model were determined according to the procedure described in detail by Wichtmann et al. (2008). The constants have been summarized by Wichtmann et al. (2007c). While $C_p = 0.59$ and $C_Y = 2.6$ were proposed to be independent of the type of sand, the following correlations of the remaining constants with index properties, in particular with d_{50}, C_u and the minimum void ratio $e_{\min}$ (determined according to DIN 18126) could be established:

$$C_e = 0.89\, e_{\min} \tag{6}$$

$$C_{N1} = 0.0002\, \exp(-0.65\, d_{50})\, \exp(0.91\, C_u) \tag{7}$$

$$C_{N2} = 0.95\, \exp(0.33\, d_{50})\, \exp(-0.90\, C_u) \tag{8}$$

$$C_{N3} = 0.00003\, \exp(-0.69\, d_{50})\, \exp(0.26\, C_u) \tag{9}$$

A set of constants may be roughly estimated from Eqs. (6) to (9). If cyclic triaxial devices are available, a set of constants may be obtained with little effort by estimating $C_p = 0.59$, $C_Y = 2.6$ and C_e from Eq. (6) and by performing only one test in order to find the constants C_{N1} to C_{N3}.

5 "ELASTIC" STIFFNESS

The components of the isotropic elastic stiffness tensor E have been formulated by comparing the rates of volumetric strain $\dot{\varepsilon}_v^{\text{acc}}$ in drained cyclic triaxial tests and the rates of pore water pressure $\dot{u}$ in undrained cyclic tests (Wichtmann et al., 2007c). Two specimens were prepared with similar relative densities and consolidated under the same isotropic stress. Afterwards the specimens were subjected to a drained or undrained cyclic loading, respectively. Such tests were performed on 15 pairs of samples. The initial pressure 50 kPa $\leq p_0 \leq$ 300 kPa and the amplitude ratio $0.2 \leq q^{\text{ampl}}/p_0 \leq 0.4$ were varied.

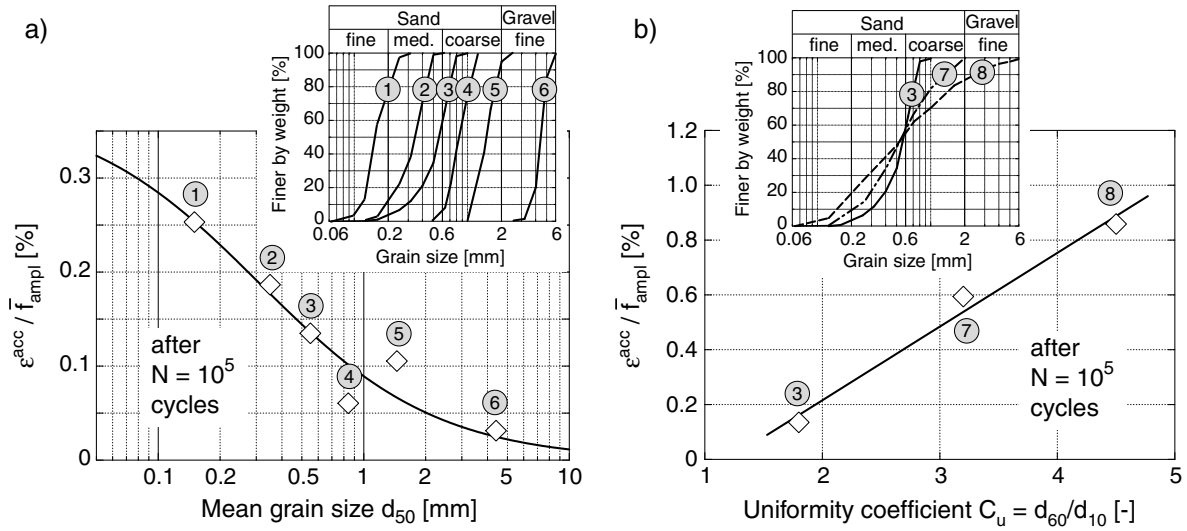

Fig. 2: *Residual strain in cyclic triaxial tests after* 10^5 *cycles in dependence on a) mean grain size* d_{50} *and b) uniformity coeffi cient* C_u

The bulk modulus was calculated from $K = \dot{u}/\dot{\varepsilon}_v^{\text{acc}}$ with $\dot{u}$ and $\dot{\varepsilon}_v^{\text{acc}}$ being the rates from the undrained and the drained test with similar values of I_{D0}, p_0 and q^{ampl}. Correction factors were applied to K in order to consider the different evolution of strain amplitude, void ratio and effective average mean pressure with the number of cycles N in the drained and the undrained test, respectively. The bulk modulus during the first cycles could be approximated by

$$K \;=\; 542 \cdot p_{\text{atm}}^{1-0.31} \cdot p^{0.31} \tag{10}$$

with a reference pressure p_{atm} = 100 kPa, but for all pairs of drained and undrained tests K was found to decrease significantly with N (Wichtmann et al., 2007c). The reasons for these observations (membrane penetration effects may contribute) are not well understood yet and need further investigations. At present it is recommended to use an isotropic E with K according to Eq. (10) and with $\nu = 0.2$.

6 NEW IDEAS FOR AN AMPLITUDE DEFINITION FOR COMPLEX 6-DIMENSIONAL STRAIN LOOPS

A procedure for the handling of complex 6-D strain loops has been proposed by Niemunis et al. (2007). For practical applications in soil mechanics the detrended strain path $\varepsilon_{ij}(t)$ is assumed to be a superposition of individual harmonic oscillations. The harmonic oscillations can be distinguished judging by the frequency f_K (or angular velocity $\omega_K = 2\pi f_K$). From each of six components $\varepsilon_{ij}(t)$ of the strain path we pick up a portion which corresponds to a common dominant frequency f_K. The componentwise sum of these six signals constitutes a *harmonic oscillation*. In general it is a 6-dimensional ellipse in the strain space. In this Section the oscillations are numbered with the capital letter K. The signal $\varepsilon_{ij}(t)$ is approximated as a sum of M oscillations:

$$\varepsilon_{ij}(t) \;\approx\; \sum_{K=1}^{M} \varepsilon_{ij}^{K}(t) = \sum_{K=1}^{M} \varepsilon_{ij}^{\text{ampl}K} \sin(\omega^K t + \varphi_{ij}^K) \tag{11}$$

A spectral analysis is used for filtering out the individual strain components ε_{ij}^K corresponding to the same angular velocity ω^K and gathering them into common oscillations. This needs to be done

only for several dominant frequencies f^K with $K = 1, 2, \ldots$ for which the strain amplitudes $\varepsilon_{ij}^{\mathrm{ampl}K}$ are large. Since the square of the amplitude dictates the accumulation rate the impact of smaller amplitudes becomes negligible. The determination of the amplitudes $\varepsilon_{ij}^{\mathrm{ampl}K}$ and the phase shifts φ_{ij}^{K} is explained in detail by Niemunis et al. (2007). Having filtered out the components for an oscillation K the remaining oscillations are selected analogously using the *reduced* signal (Niemunis et al., 2007). The fatigue load contributions from the individual oscillations i.e. the size of the amplitude $\varepsilon^{\mathrm{ampl}K} = \|\boldsymbol{\varepsilon}^{\mathrm{ampl}K}\|$ and the number of cycles N enter the fatigue loading independently. The experimental proof of the outlined procedure will be given in future.

7 FE EXAMPLE: STATICALLY INDETERMINATE STRUCTURE ON NON-HOMOGENEOUS SOIL

The geometry of the calculated statically indeterminate structure is presented in Figure 3. The random spatial distribution of void ratio has been generated using the Latin-Hypercube algorithm (Florian, 1992). The procedure has been explained in detail by Niemunis et al. (2005a). Ten random fields $e(\mathbf{x})$ have been generated with a correlation length L = 2 m. The field $e(\mathbf{x})$ shown in Figure 3 has been used for all calculations within the present study.

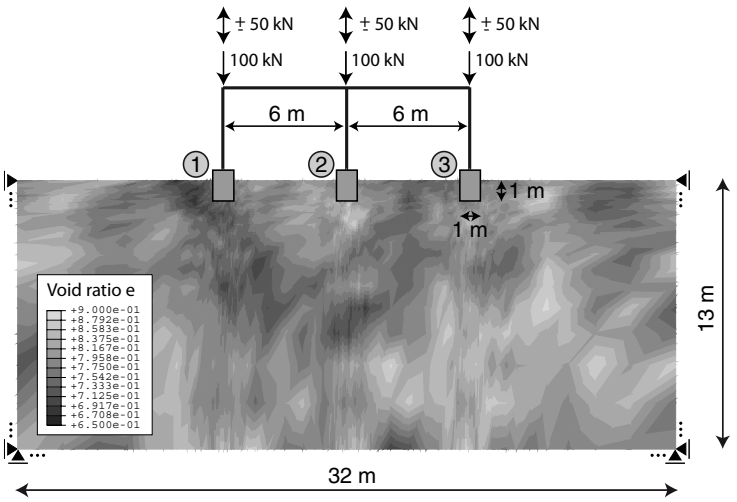

Fig. 3: *Dimensions of the calculated statically indeterminate structure and field of void ratio* $e(\mathbf{x})$

Figure 4 presents the results of a calculation without any bending stiffness $EI \approx 0$ of the frame and applying the load 100 ± 50 kN directly on the foundations. Control cycles were introduced at $N = 10^2$, 10^3 and 10^4 in order to update the amplitude field $\varepsilon^{\mathrm{ampl}}(\mathbf{x})$. The foundation in the middle shows the largest settlement since its subsoil is looser than those of its neighbours. The amplitudes of settlement stay almost constant during the 10^5 load cycles.

An analogous calculation with a relatively stiff frame ($EI = 3000$ MPa m^4/m) is shown in Figure 5. The load 100 ± 50 kN has been applied at the top of each column (Figure 3). Due to the load redistribution and reduced settlement (compared to the soft frame, Figure 5c), a stress relaxation takes place in the soil under the middle foundation. While the contact normal force under the middle column significantly decreases with N it consequently increases under the outer columns (Figure 5a). For $N > 10^4$ even tension forces occur in the middle column which are carried by friction. The middle foundation loses its function resulting in large bending moments in the structure. The rate of stress relaxation significantly increases after each control cycle because the strain amplitudes in the soil do so. This is due to a decrease of the effective stress and thus stiffness while the load amplitudes

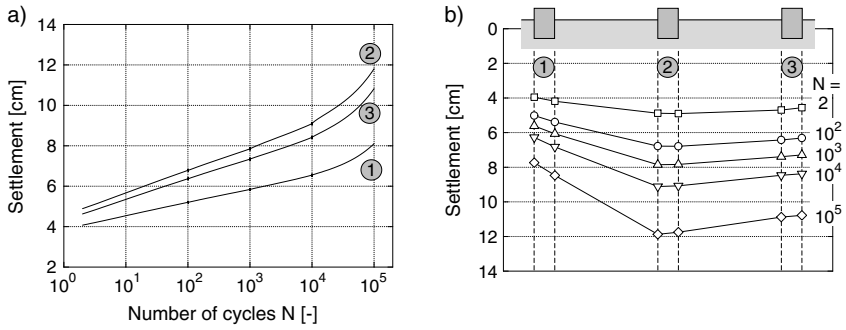

Fig. 4: *Results of FE calculations with a frame with bending stiffness $EI \approx 0$: a) settlement curves $s(N)$ and b) sagging for different N-values*

do not significantly change with N. An additional acceleration of accumulation may be due to an increase of $\dot{\varepsilon}^{\text{acc}}$ with decreasing p^{av} (Section 2). The curves in Figure 5a show that more than the three actually used control cycles are necessary.

For a monotonous loading a large settlement of a foundation and the accompanying re-distribution of loading would lead to a plasticifcation of the soil below the neighbouring foundations. The resulting increase of settlement of these foundations would equalize the differential settlement. This good-natured behaviour is not observed for cyclic loading. A decrease of load may even accelerate the accumulation of settlement or the stress relaxation (positive feedback between the settlement and the settlement rate).

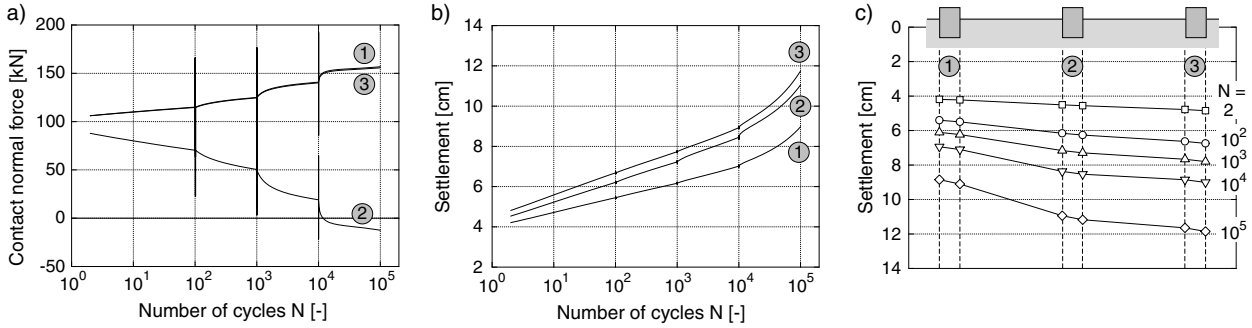

Fig. 5: *Results of FE calculations with a relatively stiff frame ($EI = 3000$ MPa m^4/m): a) development of normal force with N, b) settlement curves $s(N)$ and c) sagging for different N-values*

8 SUMMARY AND CONCLUSIONS

Recent experimental findings and developments of the high-cycle accumulation (HCA) model for sand (Niemunis et al., 2005b) have been presented. It has been demonstrated that Miner's rule is approximately applicable to sand. A simplified procedure for the determination of the material constants of the HCA model has been proposed based on approx. 200 cyclic triaxial tests. Correlations of the constants with index properties have been established. The elastic stiffness E of the HCA model has been studied comparing results of drained and undrained cyclic triaxial tests. The unexpected decrease of the bulk modulus $K = \dot{u}/\dot{\varepsilon}_v^{\text{acc}}$ with the number of cycles N needs further investigations. New ideas for an amplitude definition for complex six-dimensional strain loops have been presented. Their experimental verification will follow. An FE example with a statically indeterminate structure on an inhomogeneous soil under cyclic loading was presented. A positive feedback effect between

the settlement and the settlement rate has been demonstrated.

ACKNOWLEDGEMENT

The authors are indepted to German Research Council (DFG) for the financial support within the Collaborate Research Centre SFB 398 ”Lifetime oriented design concepts” (project A8).

REFERENCES

Florian, A. 1992. An effcient sampling scheme: Updated latin hypercube sampling. *Probabilistic Engineering Mechanics*, 2(7):123–130.

Miner, M. 1945. Cumulative damage in fatigue. *Transactions of the American Society of Mechanical Engineering*, 67:A159–A164.

Niemunis, A., Wichtmann, T., Petryna, Y. & Triantafyllidis, Th. 2005a. Stochastic modelling of settlements due to cyclic loading for soil-structure interaction. In G. et al. Augusti, editor, *Proc. of 9th International Conference on Structural Safety and Reliability, ICOSSAR 2005, Rom*, page 263.

Niemunis, A., Wichtmann, T. & Triantafyllidis, Th. 2005b. A high-cycle accumulation model for sand. *Computers and Geotechnics*, 32(4):245–263.

Niemunis, A., Wichtmann, T. & Triantafyllidis, Th. 2007. On the defi nition of the fatigue loading for sand. In *International Workshop on Constitutive Modelling - Development, Implementation, Evaluation, and Application, 12-13 January 2007, Hong Kong*.

Wichtmann, T. 2005. Explicit accumulation model for non-cohesive soils under cyclic loading. Dissertation, Schriftenreihe des Institutes für Grundbau und Bodenmechanik der Ruhr-Universität Bochum, Issue No. 38.

Wichtmann, T., Niemunis, A. & Triantafyllidis, Th. 2005a. Strain accumulation in sand due to cyclic loading: drained triaxial tests. *Soil Dynamics and Earthquake Engineering*, 25(12):967–979.

Wichtmann, T., Niemunis, A., Triantafyllidis, Th. & Poblete, M. 2005b. Correlation of cyclic preloading with the liquefaction resistance. *Soil Dynamics and Earthquake Engineering*, 25(12):923–932.

Wichtmann, T., Niemunis, A., Triantafyllidis, Th. 2006a. Experimental evidence of a unique flow rule of non-cohesive soils under high-cyclic loading. *Acta Geotechnica*, 1(1):59–73.

Wichtmann, T., Niemunis, A., Triantafyllidis, Th. 2006b. Gilt die Miner’sche Regel für Sand? *Bautechnik*, 83 (5):341–350.

Wichtmann, T., Niemunis, A., Triantafyllidis, Th. 2007a. On the influence of the polarization and the shape of the strain loop on strain accumulation in sand under high-cyclic loading. *Soil Dynamics and Earthquake Engineering*, 27(1):14–28.

Wichtmann, T., Niemunis, A., Triantafyllidis, Th. 2007b. Strain accumulation in sand due to cyclic loading: drained cyclic tests with triaxial extension. *Soil Dynamics and Earthquake Engineering*, 27(1):42–48.

Wichtmann, T., Niemunis, A., Triantafyllidis, Th. 2007c. Recent advances in constitutive modelling of compaction of granular materials under cyclic loading. In N. Bazeos, D.C. Karabalis, D. Polyzos, D.E. Beskos, and J.T. Katsikadelis, editors, *Proc. of 8th HSTAM International Congress on Mechanics, Patras, Greece 12 14 July*, volume 1, pages 121–136.

Wichtmann, T., Niemunis, A., Triantafyllidis, Th. 2008. On the determination of the constants for a high-cycle model for sand. In *International Conference on Numerical Computation in Geotechnical Engineering (NUCGE 2008), Skikda, Algeria, 27-29 October*.